Separation and Purification Technology 135 (2014) 259–267

Contents lists available at ScienceDirect

Separation and Purification Technology

journal homepage: www.elsevier.com/locate/seppur

Design of novel aqueous micellar two-phase systems using ionic liquids as co-surfactants for the selective extraction of (bio)molecules

Filipa A. Vicente [a,c], Luciana P. Malpiedi [b,c], Francisca A. e Silva [a], Adalberto Pessoa Jr. [c], João A.P. Coutinho [a], Sónia P.M. Ventura [a,*]

[a] CICECO, Departamento de Química, Universidade de Aveiro, 3810-193 Aveiro, Portugal
[b] Departamento de Química-Física, Universidad Nacional de Rosario, Rosario, Argentina
[c] Faculdade de Ciências Farmacêuticas, Universidade de São Paulo, São Paulo, Brazil

ARTICLE INFO

Article history:
Received 7 May 2014
Received in revised form 25 June 2014
Accepted 28 June 2014
Available online 28 August 2014

Keywords:
Aqueous micellar two-phase system
Triton X-114
Ionic liquids
Co-surfactant
Selective extraction

ABSTRACT

Aqueous micellar two-phase systems (AMTPS) using surfactants have been widely applied as an advantageous extraction technology for a wide range of (bio)molecules. When composed by two surfactants (the second one used as the co-surfactant), the extractive performance of such systems is considerably boosted. In this context, this work looks at ionic liquids (ILs) as a new class of tunable co-surfactants to be applied in AMTPS. Three distinct families of ILs, namely imidazolium, phosphonium and quaternary ammonium were applied in the design of the binodal curves of novel AMTPS based on the nonionic surfactant Triton X-114. On these systems it was investigated the impact of the IL absence/presence, concentration and structural features on the binodal curves behavior. Aiming at evaluating their applicability as extraction systems, partitioning studies of two targeted (bio)molecules, namely the protein Cytochrome c (Cyt c) and the dye/model drug Rhodamine 6G (R6G), were carried out. It is shown that the presence of ILs as co-surfactants is able not only to enhance the partition coefficients of Cyt c (indicated as $\log K_{Cyt\ c}$) from -0.59 ± 0.12 up to -1.51 ± 0.14, but also to improve the selectivity parameter ($S_{R6G/Cyt\ c}$) from 925.25 up to 3418.89. The results here obtained open new perspectives in the design of liquid–liquid separation processes, transversal to various fields and a wide range of applications.

1. Introduction

During the last few years, with the appearance of new biopharmaceuticals and other complex molecules of biotechnological origin, there is a stringent need for improvements at the level of the downstream processing. While several advances in large-scale production methodologies were attained, the downstream still remains the main drawback for the scale-up of various processes towards industrial implementation. This is mainly due to technological limitations and the need for multiple unit operations to obtain a final product fulfilling the strict purity and safety requirements [1]. Chromatographic techniques are the most usual choice in these fields, owing to their simplicity, selectivity and accurate resolution; however, such methodologies present some limitations related with their scalability and economic viability [2]. Thus, there is an urgent demand for new separation/purification techniques, that present good extractive performances, as well as guarantee the chemical structure and activity of the biomolecule isolated, while maintaining the economic viability of the entire process.

Liquid–liquid extraction (LLE) has been identified as a suitable technique for downstream processes due to its simple and fast operation. Traditionally, LLE was mostly accomplished by applying environmentally nefarious and expensive organic solvents [3]. In this context, aqueous two-phase systems (ATPS) emerged as appellative types of LLE, since they are mainly composed of water and do not require the use of organic solvents in the whole process, providing mild operation conditions [4,5]. These systems consist of two aqueous-rich phases of two structurally different compounds that are immiscible above stated values of concentration, undergoing phase separation. At the end, ATPS give rise to highly flexible approaches, since a considerable array of compounds, *e.g.* polymers, salts or surfactants, can be combined in order to strategically design them to achieve high extraction and purification effectiveness, selectivities and yields [4].

Aqueous micellar two-phase systems (AMTPS) are specific types of ATPS that use surfactants and appear as promising techniques for bioseparation purposes, due to their remarkable ability of keeping the native conformations and activities of biomolecules [6],

* Corresponding author. Address: Campus Universitário de Santiago, University of Aveiro, Aveiro, Portugal. Tel.: +351 234 370200; fax: +351 234 370084.
E-mail address: spventura@ua.pt (S.P.M. Ventura).

http://dx.doi.org/10.1016/j.seppur.2014.06.045
1383-5866/

while they are migrating between the aqueous-rich coexisting phases. Surfactants are amphiphilic molecules, *i.e.* present a polar, hydrophilic and sometimes charged 'head' and a non-polar, hydrophobic 'tail'. When its concentration is above a certain value, *i.e.* the critical micelle concentration (CMC), the surfactant molecules form self-assembling aggregates [6,7]. Within micelles, each surfactant molecule displays its 'tail' in the interior, while its 'head' plays an important role in the interface between the aqueous solution and the aggregate's core [6–8]. AMTPS appear when the surfactants present in aqueous solution are able to form two macroscopic phases under specific conditions. These systems are dependent on temperature and surfactant concentration, displaying a single phase below a temperature [7], known as cloud point [9] or T_{cloud} [8], and undergoing phase separation above T_{cloud}. AMTPS are composed of two distinct phases, one micelle-rich and one micelle-poor, that can be either the top or bottom layers, depending on the surfactant adopted [6–9]. The phase separation behavior for different surfactants can be described by establishing the binodal curves, *i.e.* plotting T_{cloud} *versus* surfactant concentration, which represent the boundary between the conditions at which the system presents a single phase (below/outside the curve) or two macroscopic phases (above/inside the curve) [7]. Meanwhile, some additives, depending on their physico-chemical properties, were shown to affect the phase separation behavior of surfactant-based mixtures [10,11].

The pioneering work of Bordier [12], in which the differential partitioning of a plethora of proteins within AMTPS phases was successfully carried out, triggered the publication of many other works applying this type of systems in bioseparation. Since then, not only the separation, concentration and purification of several proteins using AMTPS were addressed [6–8,13,14], but also of a wider array of biocompounds such as viruses [6], DNA [15], bacteriocins [16], antibiotics [17] and porphyrins [18]. Moreover, Kamei and co-workers [19] focused on the balance of interactions affecting the effectiveness of such systems and proved that the electrostatic forces between biomolecules and micelles play a crucial role in the migration phenomenon in AMTPS composed of a pair of distinct surfactants; the authors brought new evidences that this technique could be an enhanced route for the selective extraction, if properly designed. Based on this concept, this work envisages the exploitation of this type of interactions in the partitioning phenomenon in AMTPS by introducing a novel class of ionic solvents – the ionic liquids (ILs). During the last decade, ILs have attracted the attention from both academia and industry in several areas of application; one of those includes the use of ILs as suitable and effective separation and purification agents in ATPS, boosting the extractive performance as well as the selectivity parameters [20]. This crescent interest relays on their unique properties, such as negligible vapor pressure, high chemical and thermal stability, non-flammability, low melting point among others [20–22]. Moreover, ILs are liquid in a wide range of temperatures and are able to solvate solutes from a broad spectrum of polarities, and owing to the countless cation/anion possible combinations their properties can be tuned to fit the specific purposes of a given application [20,21]. The application of such solvents in AMTPS can be supported by the evidence produced by Bowers et al. [23], describing the possibility of ILs to self-aggregate because when they have a long enough alkyl chain they are amphiphilic molecules. Since then, a number of authors have studied the aggregation and micelle formation of ILs in aqueous solutions [24–28], their incorporation in mixed micelles [26–34] and their contribution to the modification of the physico-chemical properties of surfactant micelles [24,26–34]. ILs with long alkyl chains were also found to be able to self-aggregate, promoting significant increments in enzymatic activity [35]. The addition of ILs to a surfactant can either decrease [26,29,31] or increase [28,32,33] the CMC and also affect the aggregation number [23,24,29], depending on the ILs structural features (alkyl side chain, cation and anion) and the surfactant head group [26,29,34]. The ILs ability to act as surfactants has been evaluated by the determination of their CMCs using several methods, such as, electric conductivity [23–25,27,29,31], surface tension [23,28,32,34], fluorescence [24,26] and isothermal titration calorimetry [25,31] measurements.

Herein, a novel class of AMTPS based on the nonionic surfactant Triton X-114 as the main surfactant, the McIlvaine buffer and ILs belonging to three distinct families, namely the imidazolium, the phosphonium and the quaternary ammonium as co-surfactants (the use of ILs as co-surfactants to form mixed micelles was already briefly described [36]) is assessed. The solubility curves of such systems were established to evaluate the impact of the presence of the IL as co-surfactant in conventional surfactant/salt-based AMTPS, as well as its concentration and structural features. Moreover the potential of these AMTPS to be used in (bio)separation processes was evaluated. They were investigated in terms of their capacity to selectively separate two model (bio)molecules: the protein Cytochrome c (Cyt c), which possesses an essential biological role and here used as a model protein [6], and Rhodamine 6G (R6G) used as a model drug [37].

2. Experimental section

2.1. Material

The imidazolium-based ILs 1-decyl-3-methylimidazolium chloride [C_{10}mim]Cl (purity >98 wt%), 1-dodecyl-3-methylimidazolium chloride [C_{12}mim]Cl (purity >98 wt%) and 1-methyl-3-tetradecylimidazolium chloride [C_{14}mim]Cl (purity >98 wt%) were acquired at Iolitec (Ionic Liquid Technologies, Heilbronn, Germany). All the phosphonium-based ILs, namely trihexyltetradecylphosphonium chloride [$P_{6,6,6,14}$]Cl (purity = 99.0 wt%), trihexyltetradecylphosphonium bromide [$P_{6,6,6,14}$]Br (purity = 99.0 wt%), trihexyltetradecylphosphonium decanoate [$P_{6,6,6,14}$][Dec] (purity = 99 wt%), trihexyltetradecylphosphonium dicyanamide [$P_{6,6,6,14}$][$N(CN)_2$] (purity = 99.0 wt%), trihexyltetradecylphosphonium bis (2,4,4-trimethylpentyl)phosphinate [$P_{6,6,6,14}$][TMPP] (purity = 93.0 wt%) and tetraoctylphosphonium bromide [$P_{8,8,8,8}$]Br (purity = 95.0 wt%) were kindly supplied by Cytec. The ammonium-based IL tetraoctylammonium bromide [$N_{8,8,8,8}$]Br (purity = 98 wt%) was purchased from Sigma–Aldrich®. The chemical structures of the cations and anions composing the list of ILs herein investigated are depicted in Fig. 1a. Triton X-114 (laboratory grade) was supplied by Sigma–Aldrich®and the McIlvaine buffer components, namely sodium phosphate dibasic anhydrous Na_2HPO_4 (purity $\geqslant$99%) and citric acid anhydrous $C_6H_8O_7$ (purity = 99.5%) were acquired at Fisher Chemical and Synth, respectively. The Cytochrome c (Cyt c) from horse heart (purity $\geqslant$95 wt%) and Rhodamine 6G (R6G) (purity $\approx$95 wt%), depicted in Fig. 1b, were both acquired at Sigma–Aldrich®.

2.2. Methods

2.2.1. Binodal curves

The binodal curves of the AMTPS composed of Triton X-114 and the McIlvaine buffer at pH 7 (82.35 mL of 0.2 M Na_2HPO_4 + 17.65 mL of 0.1 M $C_6H_8O_7$), using different ILs as co-surfactants were determined using the cloud point method, whose experimental protocol is well described in literature [38]. This methodology consists of a visual identification, while raising the temperature, of the point at which a mixture with known compositions becomes turbid and cloudy, *i.e.* T_{cloud}. Then, the experimental binodal curves are obtained by plotting the T_{cloud} *versus* the surfactant mass

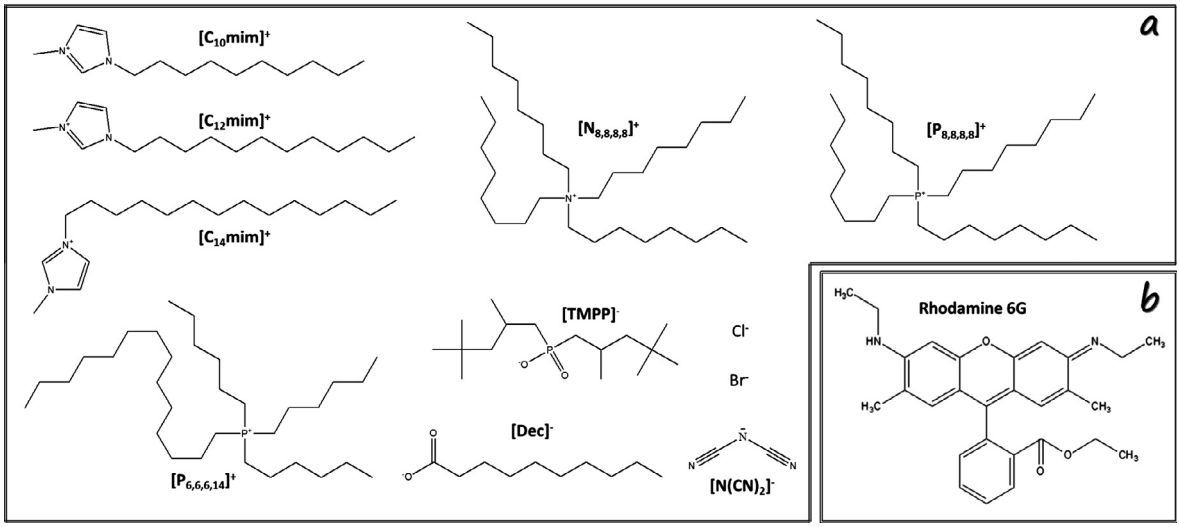

Fig. 1. Chemical structure representation of (a) cations and anions composing the ILs plus the respective abbreviations, and (b) Rhodamine 6G.

concentration. The knowledge acquired from them allows the selection of strategic mixture points which correspond to the biphasic region. This biphasic region represents the zone of temperature *versus* surfactant mass concentration where the micelles are formed. All binodal curves were determined, at least, in triplicate, and the respective standard deviations calculated and presented.

2.2.2. Partitioning studies of Cyt c and R6G by applying AMTPS

The AMTPS used in the partitioning studies of both Cyt c and R6G were gravimetrically prepared in glass tubes by weighing specific amounts of each component: 10 wt% of Triton X-114 + 0 wt%, 0.3 wt% or 0.5 wt% of each IL tested, being the McIlvaine buffer solution at pH 7 used to complete a final volume of 10 mL. To each system, the appropriate amount of each one of the model (bio)molecules was added: 10 wt% of an aqueous solution of Cyt c (*at circa* 2.0 g L^{-1}) and approximately 0.30 mg of the R6G dye powder. The systems were homogenized at least for 2 h in the freezer at 7 °C, using a tube rotator apparatus model 270 from Fanem®, avoiding the turbidity of the system. Then, the systems were left at 35 °C overnight, allowing the thermodynamic equilibrium to be reached, thus completing the separation of the phases as well as the migration of the model molecules. At the conditions adopted in the present work, the systems resulted in a micelle-rich and a micelle-poor as the bottom and top layers, respectively. Both phases were carefully separated and collected for the measurement of volume, viscosity, and quantification of the model molecules. The UV–Vis spectroscopy was elected to quantify each molecule at 409 nm for Cyt c and 527 nm for R6G, using a Molecular Devices Spectramax 384 Plus | UV–Vis Microplate Reader. The analytical quantifications were performed in triplicate and at least three parallel assays for each system were done, being the average values and the respective standard deviations presented. Possible interferences of the AMTPS components (Triton X-114, McIlvaine buffer or IL when present) within the analytical quantification method were investigated and prevented through routinely applying blank controls. Thus, the partition coefficients for Cyt c ($K_{\text{Cyt c}}$) and R6G (K_{R6G}) were calculated as the ratio between the amount of each compound present in the micelle-rich (bottom) and the micelle-poor (top) phases, as described in Eqs. (1) and (2).

$$K_{\text{Cyt c}} = \frac{[\text{Cyt c}]_{\text{Bot}}}{[\text{Cyt c}]_{\text{Top}}} \quad (1)$$

where $[\text{Cyt c}]_{\text{bot}}$ and $[\text{Cyt c}]_{\text{bot}}$ are, respectively, the concentration of Cyt c (in g L^{-1}) in the bottom and top phases.

$$K_{\text{R6G}} = \frac{\text{Abs}_{\text{Bot}}^{\text{R6G}}}{\text{Abs}_{\text{Top}}^{\text{R6G}}} \quad (2)$$

where $\text{Abs}_{\text{Bot}}^{\text{R6G}}$ and $\text{Abs}_{\text{Top}}^{\text{R6G}}$ are the absorbance data of R6G in the bottom and top phases, respectively. It should be stressed that the concentration of Cyt c in each phase was determined based on a calibration curve previously established. However, due to practical limitations that disallowed the determination of a calibration curve for R6G, the K_{R6G} was calculated having into consideration the final values of Abs in both phases. The recovery (R) parameters of each molecule towards the bottom (R_{Bot}) and the top (R_{Top}) phases were determined following Eqs. (3) and (4):

$$R_{\text{Bot}} = \frac{100}{1 + \left(\frac{1}{R_v \times K}\right)} \quad (3)$$

$$R_{\text{Top}} = \frac{100}{1 + R_v \times K} \quad (4)$$

where R_v stands for the ratio between the volumes of the bottom and top phases. Finally, the selectivity ($S_{\text{R6G/Cyt c}}$) of the AMTPS herein developed was described as the ratio between the K values found for R6G and Cyt c, as indicated in Eq. (5):

$$S_{\text{R6G/Cyt c}} = \frac{K_{\text{R6G}}}{K_{\text{Cyt c}}} \quad (5)$$

2.2.3. Viscosity measurements of both phases

The viscosity was measured using an automated SVM 3000 Anton Paar rotational Stabinger viscosimeter-densimeter at 25 °C and at atmospheric pressure for each top and bottom phases of the entire set of AMTPS studied.

3. Results and discussion

3.1. Design of the binodal curves with ILs acting as co-surfactants

The first step of this work consisted on the determination of the binodal curves of AMTPS with several ILs as co-surfactants [36], which knowledge is essential not only to perform the partitioning studies, but also to optimize the operational conditions of the

separation process. Therefore, the binodal curves were established through visual identification of the T_{cloud} for all the mixtures composed of Triton X-114, McIlvaine buffer, either in the absence or presence of IL. During the binodal curves determination, the effect of the presence of different ILs as co-surfactants was assessed, and with it, several ILs chemical features were strategically considered, namely the alkyl side chain length, the anion structure and the cation conformation, and the ILs' mass concentration, being their impact minutely discussed in the next sections.

3.1.1. Effect of the ILs' presence

A set of ten distinct ILs, belonging to the imidazolium ($[C_n mim]^+$ with n = 10, 12 and 14), phosphonium ($[P_{6,6,6,14}]^+$ and $[P_{8,8,8,8}]^+$) and ammonium ($[N_{8,8,8,8}]^+$) families, were applied as co-surfactants in AMTPS based in Triton X-114 and the McIlvaine buffer. The experimental binodal curves obtained are depicted in Figs. 2 and 3, revealing that the presence of different ILs highly affects the phase separation phenomenon either incrementing or decreasing the T_{cloud}. In this sense, ILs can be divided into two main groups related with the impact on phase formation, when compared to the original AMTPS (Triton X-114 + McIlvaine buffer). The first group involves the imidazolium-based ILs, more hydrophilic, which produce an increase in the T_{cloud}. The second group, which covers the phosphonium- and quaternary ammonium-based ILs, more hydrophobic, that induce significant reductions in the T_{cloud} [39]. The opposite trends here verified are attributed to the main interactions competing and governing the phase separation phenomenon in these specific AMTPS. Actually, this phenomenon is complex and is strongly dependent of the balance involving the hydration degree of the surfactant chain and the electrostatic interactions among the charged head group [40]. Concerning the first group, it can be related with the greater hydration shell present around the imidazolium-based ILs and consequent higher energy required to separate the system into two macroscopic phases [33] or with the IL head group that may charge the micellar surface, thus generating electrostatic repulsion between them [41]. In this manner, ILs with stronger hydrophobic nature may lead to smaller micellar hydration shells enhancing the ability to undergo phase separation at lower temperatures [42]. The picture emerging from these data indicates that the most hydrophobic ILs, independently of their concentration, seem to be more advantageous co-surfactants from an operational point of view, since lower temperatures are better conditions for (bio)separation processes.

3.1.2. Effect of the ILs' structural features

Aiming at designing more efficient ILs to be applied as co-surfactants in Triton X-114 + McIlvaine buffer-based AMTPS, several modifications at the level of the alkyl side chain, the anion moiety and the cation core were conducted. In order to address the impact of the alkyl side chain of the cation on the phase separation behavior, three $[C_n mim]Cl$-based ILs were selected, varying their n value from 10 to 14 carbon atoms. Their comparative representation is depicted in Figs. 2 and 3 and it is possible to observe that, independently of the mass concentration of IL added, 0.3 wt% or 0.5 wt%, the capability to generate two phases increases according to the trend $[C_{10}mim]Cl < [C_{12}mim]Cl < [C_{14}mim]Cl$ – *i.e.* resulting from the increasing hydrophobicity of the IL. This increasing ability to create AMTPS is a result from the lower number of water molecules around the micelles hampering their grouping in one phase, leading to less energy requirements to undergo phase separation and, consequently, lower T_{cloud} [43], which is in agreement with evidences found in literature, related with the easier aggregation of the molecules with longer alkyl chain lengths (lower Gibbs energy) [24] and with the benign impact of the lipophilicity on the T_{cloud} [25]. As expected, this effect is even stronger for $[P_{6,6,6,14}]Cl$, due to its enhanced hydrophobicity.

The influence of the anion moiety on the coexistence curves was addressed by using five different ILs sharing the $[P_{6,6,6,14}]^+$ cation, namely $[P_{6,6,6,14}]Cl$, $[P_{6,6,6,14}]Br$, $[P_{6,6,6,14}][Dec]$, $[P_{6,6,6,14}][N(CN)_2]$ and $[P_{6,6,6,14}][TMPP]$. This group of ILs induces a decrease in T_{cloud} of the Triton X-114 + McIlvaine buffer-based AMTPS, as aforementioned; however, the intensity of this behavior depends on the anion nature. The graphical representation of such binodal curves is reported in Figs. 2 and 3 in the insets. Apart from the fact that at higher IL mass concentrations, the anion influence is scattered

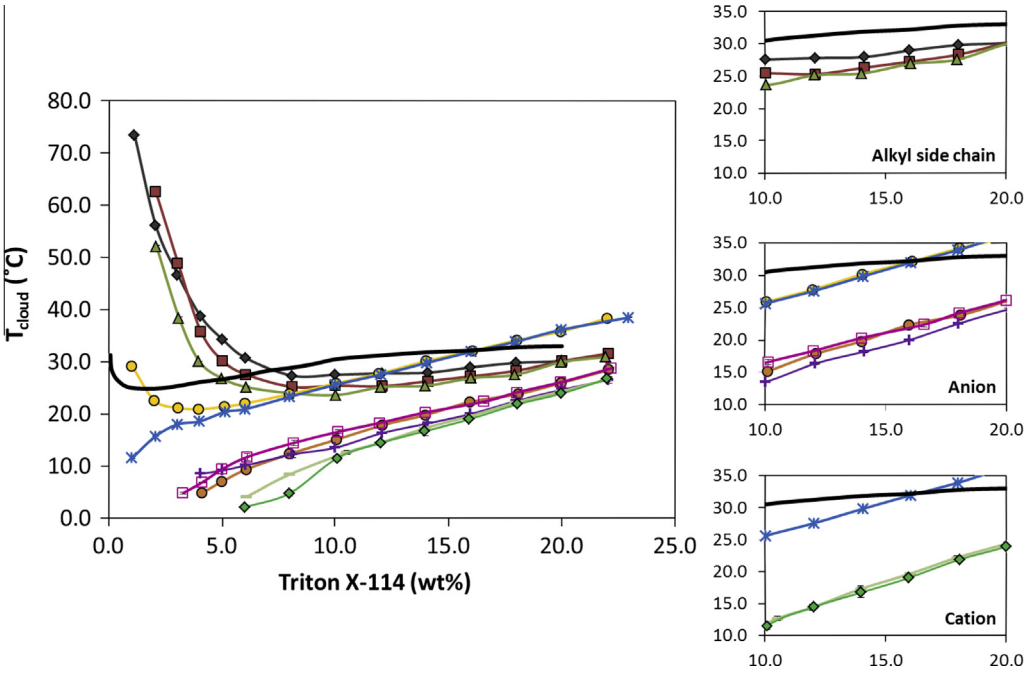

Fig. 2. Binodal curves for the studied ILs at 0.3 wt%: —, without IL; ◆, $[C_{10}mim]Cl$; ■, $[C_{12}mim]Cl$; ▲, $[C_{14}mim]Cl$; ●, $[P_{6,6,6,14}]Cl$; ✳, $[P_{6,6,6,14}]Br$; ●, $[P_{6,6,6,14}][Dec]$; +, $[P_{6,6,6,14}][N(CN)_2]$; □, $[P_{6,6,6,14}][TMPP]$; —, $[P_{8,8,8,8}]Br$; ◆, $[N_{8,8,8,8}]Br$. The effect of ILs' structural features is provided separately in the insets to facilitate the analysis.

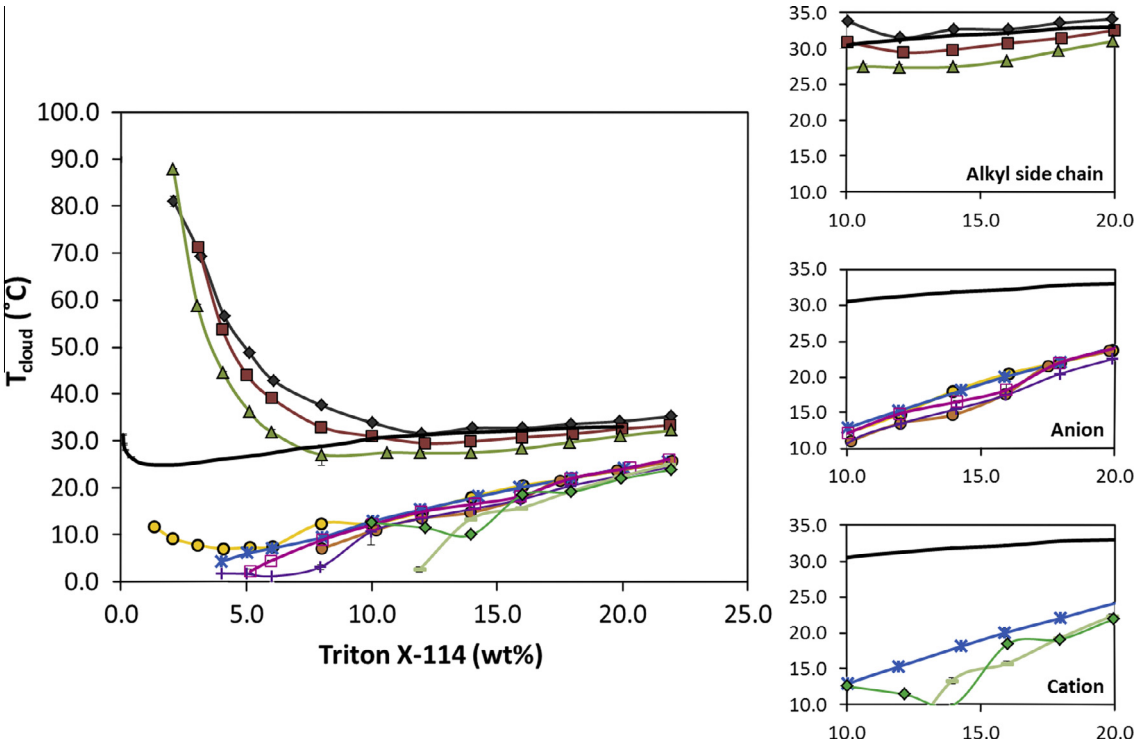

Fig. 3. Binodal curves for the studied ILs at 0.5 wt%: ——, without IL; ◆, [C_{10}mim]Cl; ■, [C_{12}mim]Cl; ▲, [C_{14}mim]Cl; ●, [$P_{6,6,6,14}$]Cl; ✳, [$P_{6,6,6,14}$]Br; ●, [$P_{6,6,6,14}$][Dec]; ┼, [$P_{6,6,6,14}$][$N(CN)_2$]; □, [$P_{6,6,6,14}$][TMPP]; ▬, [$P_{8,8,8,8}$]Br; ◆, [$N_{8,8,8,8}$]Br. The effect of the ILs' structural features is provided separately in the insets to facilitate the analysis.

(Fig. 3), at 0.3 wt% of IL is possible to notice that the ability to form two phases increases in the order [$P_{6,6,6,14}$]Cl ≈ [$P_{6,6,6,14}$]Br ≪ [$P_{6,6,6,14}$][TMPP] ≈ [$P_{6,6,6,14}$][Dec] < [$P_{6,6,6,14}$][$N(CN)_2$]. This tendency shows the existence of a clear distinction between the more hydrophilic (Cl^- and Br^-) and the more hydrophobic anions ($[TMPP]^-$, $[Dec]^-$ and $[N(CN)_2]^-$). It should be stressed that, for Cl^- and Br^- at low concentrations of Triton X-114, a more prominently distinct behavior was observed being the Br^- anion responsible for major T_{cloud} decreases. This behavior could be related to the higher ability of the Br^- to reduce the surface tension [44] or to the facilitate the Br^- adsorption into the micelles surface, reducing the electrostatic repulsion [31] and thus enhancing the molecules' tendency to self-aggregate, consequently forcing the reduction of the T_{cloud} values. When concerning the behavior induced by the remaining three anions, $[Dec]^-$, $[N(CN)_2]^-$ and $[TMPP]^-$, we attribute it to the fact that both anion and cation structures composing the IL would remain as part of the micellar structure, resulting in low micellar charge and thus, low electrostatic repulsion between them [40].

Finally, some modifications at the level of the cation, beyond the more hydrophilic *vs.* the more hydrophobic nature aforementioned, were considered. Those were connected with the change of the cation symmetry (from $[P_{8,8,8,8}]^+$ to $[P_{6,6,6,14}]^+$) or variation of the central atom from a phosphorous ($[P_{8,8,8,8}]^+$) to a nitrogen ($[N_{8,8,8,8}]^+$) element. As presented in Fig. 2 (inset), it is notorious that the symmetry is favorable to induce the ability to form AMTPS. Here again, the presence of higher concentrations of IL (Fig. 3 in the inset) decreases the effect of the structural modifications. When $[P_{8,8,8,8}]^+$ is compared with the $[N_{8,8,8,8}]^+$ cation, both possessing a strong hydrophobic nature, no significant differences between their T_{cloud} behavior are noticed independently of the IL mass concentration studied (Figs. 2 and 3 in the insets).

3.1.3. Effect of the IL concentration

The impact of the concentration of ILs on the T_{cloud} behavior of Triton X-114 + McIlvaine buffer AMTPS was assessed by slightly increasing it from 0.3 wt% up to 0.5 wt%. In Fig. 4, it is provided the comparison between the concentrations adopted in this study, being possible to observe, again, two distinct trends. One involving the imidazolium family (more hydrophilic nature) and other the phosphonium and quaternary ammonium chemical structures (more hydrophobic nature): higher concentration of ILs is converted either in an increase of the T_{cloud}, in the case of the imidazolium-based ILs, or in a reduction of the T_{cloud} for the phosphonium- and quaternary ammonium-based ILs. It should be pointed out that this change in T_{cloud} is relevant from both operational and economic points of view since very low amounts of ILs (used as co-surfactant) can significantly modify the T_{cloud} of the AMTPS. Even low amounts of [$C_n$mim]Cl-based ILs may be used to enhance

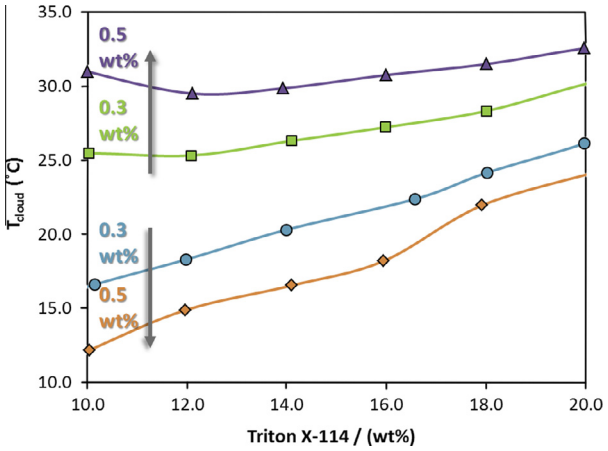

Fig. 4. Influence of the ILs' mass concentration on the T_{cloud} of AMTPS using more hydrophilic (imidazolium-based) or more hydrophobic (phosphonium-based) ILs: ■, [C_{12}mim]Cl at 0.3 wt%; ▲, [C_{12}mim]Cl at 0.5 wt%; ●, [$P_{6,6,6,14}$][TMPP] at 0.3 wt%; ◆, [$P_{6,6,6,14}$][TMPP] at 0.5 wt%. [C_{12}mim]Cl and [$P_{6,6,6,14}$][TMPP] were selected as examples to indicate the common trend for both distinct groups of ILs.

Table 1
Logarithm function of $K_{Cyt\ c}$ and K_{R6G} by the application of all AMTPS studied, at weight fraction composition of 10 wt% of Triton X-114 and 0, 0.3 or 0.5 wt% of IL.

$$K_{R6G} = \frac{Abs^{R6G}{}_{Bot}}{Abs^{R6G}{}_{Top}} \qquad K_{Cyt\ c} = \frac{[Cyt\ c]_{Bot}}{[Cyt\ c]_{Top}}$$

Bottom (Micelle-rich) Phase ← Log K_{R6G} | Log $K_{Cyt\ c}$ → Top (Micelle-poor) Phase

	IL concentration			
	0.3 wt%	0.5 wt%	0.3 wt%	0.5 wt%
no IL	2.39 ± 0.30		-0.59 ± 0.12	
[C_{10}mim]Cl	2.14 ± 0.11	1.55 ± 0.06	-0.52 ± 0.02	-0.24 ± 0.04
[C_{12}mim]Cl	1.79 ± 0.10	1.99 ± 0.04	-0.68 ± 0.04	-0.43 ± 0.05
[C_{14}mim]Cl	2.65 ± 0.00	1.90 ± 0.14	-0.69 ± 0.02	-0.52 ± 0.05
[$P_{6,6,6,14}$]Cl	2.54 ± 0.02	2.16 ± 0.06	-0.82 ± 0.04	-0.90 ± 0.04
[$P_{6,6,6,14}$]Br	2.39 ± 0.05	2.07 ± 0.13	-0.85 ± 0.06	-1.02 ± 0.01
[$P_{6,6,6,14}$][Dec]	2.25 ± 0.24	2.47 ± 0.10	-0.84 ± 0.13	-1.02 ± 0.07
[$P_{6,6,6,14}$][$N(CN)_2$]	2.02 ± 0.10	---	-0.96± 0.28	---
[$P_{6,6,6,14}$][TMPP]	2.21 ± 0.21	2.13 ± 0.04	-1.03 ± 0.07	-0.90 ± 0.15
[$P_{8,8,8,8}$]Br	2.13 ± 0.04	---	-1.08 ± 0.13	-1.51 ± 0.14
[$N_{8,8,8,8}$]Br	1.70 ± 0.01	---	-0.56 ± 0.02	---

the AMTPS performance, making them promising alternative approaches despite the higher T_{cloud} observed, for thermal stable molecules since the biphasic region is increased when compared to the AMTPS without IL, thus offering more appealing extraction conditions.

3.2. Application of the designed AMTPS to the selective extraction of Cyt c and R6G

The separation of Cyt c and R6G was attempted by applying these novel AMTPS using ILs as co-surfactants. The partitioning studies of these molecules were performed using AMTPS composed of 10 wt% of Triton X-114 in the absence and presence of 0.3 wt% and 0.5 wt% of ILs. Being important from a technological point of view, a characterization of the viscosity of the resulting phases which is reported in Table S.1 at the Supporting Information file was carried out. The results indicate that the presence of the ILs contributes to slightly reduce the viscosity of the bottom phase (micelle-poor phase) in most of the AMTPS.

The results regarding the partition behavior of the targeted molecules are reported in Table 1. It should be mentioned that in some cases, experimental limitations precluded the execution of the partitioning studies hindering the determination of partition coefficients and other parameters. It is clearly observed in the results obtained the preferential migration of Cyt c to the micelle-poor phase ($\log K_{Cyt\ c} < 0$), while the R6G is migrating to the micelle-rich phase ($\log K_{R6G} > 0$). These opposite migration tendencies can be easily understood based on a balance involving hydrophobic, electrostatic and excluded-volume interactions between the targeted molecules and the micelles. As the Cyt c is a hydrophilic protein, it presents higher affinity for the more hydrophilic layer (micelle-poor phase), which is in close agreement with literature [12]. Also, its isoelectric point – 10.65 [45] – is higher than the pH herein adopted (McIlvaine buffer at pH 7), meaning that the protein is positively charged under this set of process conditions. In this sense, electrostatic interactions seem to play an important role in the partition of Cyt c, since the IL, especially its cation, may force the protein migration towards the micelle-poor layer. Moreover, excluded-volume interactions may also interfere in the partition tendency of Cyt c, especially for higher micelle concentrations that lead to lower volume available in the micelle-rich layer, forcing its migration towards the micelle-poor phase. Meanwhile, R6G is migrating preferentially for the micelle-rich phase, since this small molecule [46] is a neutral species at pH 7; in this case, hydrophobic interactions are controlling the molecule partitioning behavior. A more detailed discussion can be performed by carefully analyzing the impact of different conditions (IL's nature and concentration) on the partitioning of Cyt c. When taking a closer look at the [$C_n$mim]Cl-based ILs as co-surfactants, it is possible to conclude that the migration increases with the elongation of the alkyl chain length (at 0.3 wt% of IL is $-0.52 \pm 0.02 < \log K_{Cyt\ c} < -0.69 \pm 0.02$ and at 0.5 wt% is $-0.24 \pm 0.04 < \log K_{Cyt\ c} < -0.52 \pm 0.05$), as shown in previous studies [47]. This behavior can be justified by the intensification of the excluded-volume interactions as the ILs' hydrophobicity increases [8,27]. When the concentration of the entire series of [$C_n$mim]Cl-based ILs increases to 0.5 wt%, the $K_{Cyt\ c}$ decreases (for example for [C_{10}mim]Cl, log $K_{Cyt\ c}$ varies from -0.52 ± 0.02 to -0.24 ± 0.04), probably as a result of operational limitations related with the proximity between the separation temperature (35 °C) and the T_{cloud} (33.82 ± 0.06 °C). Finally, in presence of the phosphonium-based ILs, especially 0.5 wt% of [$P_{8,8,8,8}$]Br, the protein is even more forced to migrate towards the micelle-poor phase ($\log K_{Cyt\ c} = -1.51 \pm 0.14$). Besides, and contrarily to the behavior

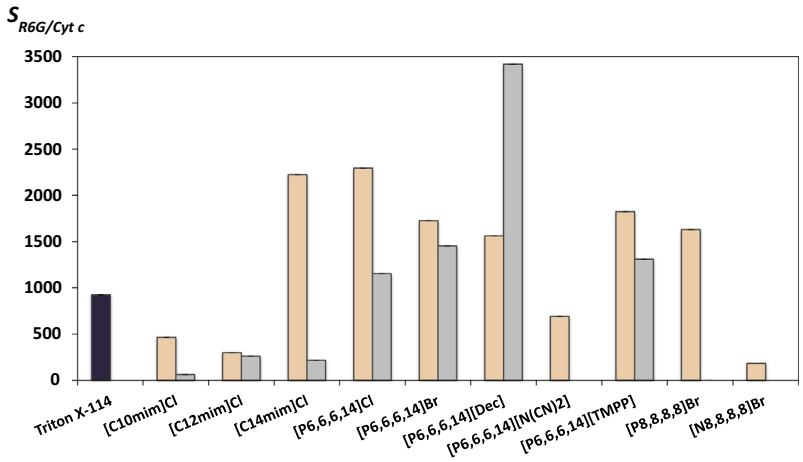

Fig. 5. Selectivity results obtained through the application of all AMTPS studied for the extraction of R6G and Cyt c: , 0.3 wt% of IL; , 0.5 wt% of IL, the color of triton X-114 (without IL).

observed with the [$C_n$mim]Cl-based ILs, increasing the concentration of IL, the $K_{Cyt\ c}$ is also increasing (*e.g.* for [$P_{8,8,8,8}$]Br the $\log K_{Cyt\ c}$ varies from -1.08 ± 0.13 to -1.51 ± 0.14). Again, these facts are corroborating the strong dependence on the hydrophobic character of the ILs, which may increase the micelles concentration, employing a more pronounced excluded-volume effect on the protein. In addition, the recovery values (regarding the phase where each molecule is more concentrated), reported in Fig. S.1 at Supporting Information file are corroborating the opposite preferential migration of Cyt c to the micelle-poor phase ($18.04 \pm 2.80\% < R_{Top} < 98.42 \pm 0.54\%$) and R6G to the micelle-rich phase ($96.12 \pm 0.15\% < R_{Bot} < 99.70 \pm 0.19\%$). It should be noted that the low R_{Top} values obtained in presence of the [$C_n$mim]Cl-based ILs are only related with the more deficient re-concentration of the Cyt c in one phase (K closer to the unit). As already described, it is notorious from the results of Table 1 that, two distinct mechanisms explain the migration of the molecules here investigated, independently of the presence of ILs as co-surfactants. However, the results of the same figure also suggest that, these partition phenomena are significantly improved by the addition of small amounts of the ILs studied. In fact, the partition of Cyt c in the conventional AMTPS ($\log K_{Cyt\ c} = -0.59 \pm 0.12$), is less pronounced when compared to the novel ones (at 0.3 wt% of IL is $-0.52 \pm 0.02 < \log K_{Cyt\ c} < -1.08 \pm 0.13$ and at 0.5 wt% of IL is $-0.24 \pm 0.04 < \log K_{Cyt\ c} < -1.51 \pm 0.14$). Indeed, the use of ILs as co-surfactants truly enhances the extractive performance of these systems; still, when applying either [C_{10}mim]Cl or [$N_{8,8,8,8}$]Br at 0.3 wt% and the [$C_n$mim]Cl series at 0.5 wt% the partition can be decreased ($-0.24 \pm 0.04 < \log K_{Cyt\ c} < -0.56 \pm 0.02$).

Finally, the preferential migration of the targeted molecules towards opposite phases of the AMTPS herein established can be reliably translated by means of their selectivity parameter ($S_{R6G/Cyt\ c}$). The results obtained are reported in Fig. 5 (and Fig. S.2 in the Supporting Information file) and remarkably suggest that the presence of ILs has a significant impact on the selectivity of this type of systems. In fact, when comparing the $S_{R6G/Cyt\ c}$ of the conventional AMTPS based in Triton X-114 + McIlvaine buffer with the novel class possessing ILs acting as co-surfactant, an almost 4-fold enhancement, from 925.25 up to 3418.89, is achieved. Meanwhile, the results of Fig. 5 also suggest that the most advantageous $S_{R6G/Cyt\ c}$ conditions were achieved applying the AMTPS containing 0.3 wt% of either [C_{14}mim]Cl ($S_{R6G/Cyt\ c} = 2224.06$) or [$P_{6,6,6,14}$]Cl ($S_{R6G/Cyt\ c} = 2295.81$) and 0.5 wt% of [$P_{6,6,6,14}$][Dec] ($S_{R6G/Cyt\ c} = 3418.89$). The selective nature is also visually proved as depicted in Fig. S.2 provided in the supporting information file.

Although the studies focusing on the partitioning of either R6G or Cyt c are limited, the performance of this novel process is here compared with other types of ATPS. The use of AMTPS with ILs as co-surfactants is capable of enhancing the extractive performance of R6G, independently of the concentration of IL employed ($1.55 \pm 0.06 < \log K_{R6G} < 2.65 \pm 0.00$ and $96.12 \pm 0.15\% < R_{Bot} < 99.70 \pm 0.19\%$), when compared to phosphonium-based ILs + tripotassium phosphate salt-based ATPS (log R6G values of -1.74, 0.56 and 0.90) [48]. On the other hand, the extractive performance of Cyt c is also here boosted ($-0.24 \pm 0.04 < \log K_{Cyt\ c} < -1.51 \pm 0.14$ and $18.04 \pm 2.80\% < R_{Top} < 98.42 \pm 0.54\%$), when compared with the results accomplished by applying either imidazolium-based IL + potassium citrate buffer-based ATPS (extraction recoveries up to 94%, by pH changes) [47] or the n-decyl tetra(ethylene oxide) + McIlvaine buffer-based AMTPS ($\log K_{Cyt\ c} \approx -0.09$) [6]. These results show that AMTPS using IL as co-surfactants are promising techniques to be successfully applied in bioseparation processes and several fields of the pharmaceutical and biotechnological industries. Having into account the industrial interest of these systems, a more profound investigation considering the recovery and recycling of the separation agents (surfactant and ILs) used is required, considering some of the techniques briefly described in literature [49,50].

4. Conclusions

This work studies for the first time the effect of ILs used as co-surfactants on the binodal curves of AMTPS composed of Triton X-114 and the McIlvaine buffer. These results clearly demonstrate that, ILs have an important effect on the T_{cloud}, *i.e.* in the binodal curves which is highly dependent on the ILs hydrophobic/hydrophilic nature. In fact, the T_{cloud} can be considerably reduced by selecting ILs possessing a hydrophobic nature, such as those belonging to the phosphonium and quaternary ammonium families.

The extraction of two model (bio)molecules, namely the Cyt c and R6G, was carried out to evaluate the partition behavior on these systems. Cyt c is shown to be concentrated on the micelle-poor phase ($\log K_{Cyt\ c} < 0$), while R6G has an extensive migration for the opposite (micelle-rich) phase ($\log K_{Cyt\ c} > 0$). These opposite behaviors are here translated by the selectivity parameter, principally for AMTPS with ILs acting as co-surfactants. In fact, it is well

demonstrated that the simple addition of a small content of these ILs has a very significant effect on improving the selective extraction of these (bio)molecules. The results herein gauged show that AMTPS with ILs as additives can be useful for the extraction and purification of (bio)molecules.

Acknowledgements

This work was also financed by FEDER through Programa Operacional Fatores de Competitividade – COMPETE and national funds through FCT – Fundação para a Ciência e Tecnologia within CICECO project - FCOMP-01-0124-FEDER-037271 (Ref. FCT PEst-C/CTM/LA0011/2013). The authors also acknowledge FCT by the doctoral and post-doctoral grants SFRH/BD/94901/2013 and SFRH/BPD/79263/2011 of F.A. e Silva and S.P.M. Ventura, respectively. The authors also thank the Santander Scholarship granted to F.A. Vicente. The authors acknowledge the financial support from FAPESP through the project FAPESP 2012/12022-6 and FAPESP, Process N° 2011/20521-0 to L.P. Malpiedi. This project was also supported by Coordenação de Aperfeiçoamento de Pessoal de Nível Superior (CAPES) and Conselho Nacional de Desenvolvimento Científico e Tecnológico (CNPq) from Brazil.

Appendix A. Supplementary material

Supplementary data associated with this article can be found, in the online version, at http://dx.doi.org/10.1016/j.seppur.2014.06.045.

References

[1] E. Langer, Trends in downstream bioprocessing, BioPharm. Int. 26 (2013) 32–36.
[2] U. Gottschalk, Bioseparation in antibody manufacturing: the good, the bad and the ugly, Biotechnol. Prog. 24 (2008) 496–503.
[3] P.G. Mazzola, A.M. Lopes, F.A. Hasmann, A.F. Jozala, T.C.V. Penna, P.O. Magalhaes, C.O. Rangel-Yagui, A. Pessoa Jr., Liquid–liquid extraction of biomolecules: an overview and update of the main techniques, J. Chem. Technol. Biotechnol. 83 (2008) 143–157.
[4] J.V.D. Molino, D.de A. Viana Marques, A.P. Júnior, P.G. Mazzola, M.S.V. Gatti, Different types of aqueous two-phase systems for biomolecule and bioparticle extraction and purification, Biotechnol. Prog. 29 (2013) 1343–1353.
[5] M. Martínez-Aragón, S. Burghoff, E.L.V. Goetheer, A.B. de Haan, Guidelines for solvent selection for carrier mediated extraction of proteins, Sep. Purif. Technol. 65 (2009) 65–72.
[6] C. Liu, D.T. Kamei, J.A. King, D.I.C. Wang, D. Blankschtein, Separation of proteins and viruses using two-phase aqueous micellar systems, J. Chromatogr. B Biomed. Sci. Appl. 711 (1998) 127–138.
[7] C.-L. Liu, Y.J. Nikas, D. Blankschtein, Novel bioseparations using two-phase aqueous micellar systems, Biotechnol. Bioeng. 52 (1996) 185–192.
[8] C.O. Rangel-Yagui, A. Pessoa-Jr, D. Blankschtein, Two-phase aqueous micellar systems: an alternative method for protein purification, Brazilian J. Chem. Eng. 21 (2004) 531–544.
[9] H. Tani, T. Kamidate, H. Watanabe, Aqueous micellar two-phase systems for protein separation, Jap. Soc. Anal. Chem. 14 (1998) 875–888.
[10] T. Gu, P.A. Galera-Gómez, Clouding of Triton X-114: the effect of added electrolytes on the cloud point of Triton X-114 in the presence of ionic surfactants, Colloids Surf. A Physicochem. Eng. Asp. 104 (1995) 307–312.
[11] P. Taechangam, J.F. Scamehorn, S. Osuwan, T. Rirksomboon, Effect of nonionic surfactant molecular structure on cloud point extraction of phenol from wastewater, Colloids Surf. A Physicochem. Eng. Asp. 347 (2009) 200–209.
[12] C. Bordier, Phase separation of integral membrane proteins in Triton X-114 solution, J. Biol. Chem. 256 (1981) 1604–1607.
[13] D.T. Kamei, J.A. King, D.I.C. Wang, D. Blankschtein, Separating lysozyme from bacteriophage P22 in two-phase aqueous micellar systems, Biotechnol. Bioeng. 80 (2002) 233–236.
[14] P.M.D. Jaramillo, H.A.R. Gomes, F.G. de Siqueira, M. Homem-de-Mello, E.X.F. Filho, P.O. Magalhães, Liquid–liquid extraction of pectinase produced by Aspergillus oryzae using aqueous two-phase micellar system, Sep. Purif. Technol. 120 (2013) 452–457.
[15] F. Mashayekhi, A.S. Meyer, S.A. Shiigi, V. Nguyen, D.T. Kamei, Concentration of mammalian genomic DNA using two-phase aqueous micellar systems, Biotechnol. Bioeng. 102 (2009) 1613–1623.
[16] A.F. Jozala, A.M. Lopes, P.G. Mazzola, P.O. Magalhães, T.C.V. Penna Jr., A. Pessoa, Liquid–liquid extraction of commercial and biosynthesized nisin by aqueous two-phase micellar systems, Enzyme Microb. Technol. 42 (2008) 107–112.
[17] V.C. Santos, F.A. Hasmann, A. Converti, A. Pessoa, Liquid–liquid extraction by mixed micellar systems: a new approach for clavulanic acid recovery from fermented broth, Biochem. Eng. J. 56 (2011) 75–83.
[18] A. Tong, Y. Wu, S. Tan, L. Li, Y. Akama, S. Tanaka, Aqueous two-phase system of cationic and anionic surfactant mixture and its application to the extraction of porphyrins and metalloporphyrins, Anal. Chim. Acta 369 (1998) 11–16.
[19] D.T. Kamei, D.I.C. Wang, D. Blankschtein, Fundamental investigation of protein partitioning in two-phase aqueous mixed (nonionic/ionic) micellar systems, Langmuir 18 (2002) 3047–3057.
[20] M.G. Freire, A.F.M. Cláudio, J.M.M. Araújo, J.A.P. Coutinho, I.M. Marrucho, J.N. Canongia Lopes, L.P.N. Rebelo, Aqueous biphasic systems: a boost brought about by using ionic liquids, Chem. Soc. Rev. 41 (2012) 4966–4995.
[21] J.F. Brennecke, E.J. Maginn, Ionic liquids: innovative fluids for chemical processing, AIChE J. 47 (2001) 2384–2389.
[22] S. Aparicio, M. Atilhan, F. Karadas, Thermophysical properties of pure ionic liquids: review of present situation, Ind. Eng. Chem. Res. 49 (2010) 9580–9595.
[23] J. Bowers, C.P. Butts, P.J. Martin, M.C. Vergara-Gutierrez, R.K. Heenan, Aggregation behavior of aqueous solutions of ionic liquids, Langmuir 20 (2004) 2191–2198.
[24] J. Wang, H. Wang, S. Zhang, H. Zhang, Y. Zhao, Conductivities, volumes, fluorescence, and aggregation behavior of ionic liquids [C4mim][BF4] and [Cnmim]Br (n = 4, 6, 8, 10, 12) in aqueous solutions, J. Phys. Chem. B 111 (2007) 6181–6188.
[25] J. Łuczak, C. Jungnickel, M. Joskowska, J. Thöming, J. Hupka, Thermodynamics of micellization of imidazolium ionic liquids in aqueous solutions, J. Colloid Interface Sci. 336 (2009) 111–116.
[26] M. Blesic, M.H. Marques, N.V. Plechkova, K.R. Seddon, L.P.N. Rebelo, A. Lopes, Self-aggregation of ionic liquids: micelle formation in aqueous solution, Green Chem. 9 (2007) 481–490.
[27] Z. Miskolczy, K. Sebők-Nagy, L. Biczók, S. Göktürk, Aggregation and micelle formation of ionic liquids in aqueous solution, Chem. Phys. Lett. 400 (2004) 296–300.
[28] F. Comelles, I. Ribosa, J.J. González, M.T. Garcia, Interaction of nonionic surfactants and hydrophilic ionic liquids in aqueous solutions: can short ionic liquids be more than a solvent?, Langmuir 28 (2012) 14522–14530.
[29] K. Behera, S. Pandey, Interaction between ionic liquid and zwitterionic surfactant: a comparative study of two ionic liquids with different anions, J. Colloid Interface Sci. 331 (2009) 196–205.
[30] K. Singh, D.G. Marangoni, J.G. Quinn, R.D. Singer, Spontaneous vesicle formation with an ionic liquid amphiphile, J. Colloid Interface Sci. 335 (2009) 105–111.
[31] N.A. Smirnova, A.A. Vanin, E.A. Safonova, I.B. Pukinsky, Y.A. Anufrikov, A.L. Makarov, Self-assembly in aqueous solutions of imidazolium ionic liquids and their mixtures with an anionic surfactant, J. Colloid Interface Sci. 336 (2009) 793–802.
[32] L.G. Chen, H. Bermudez, Charge screening between anionic and cationic surfactants in ionic liquids, Langmuir 29 (2013) 2805–2808.
[33] R. Pramanik, S. Sarkar, C. Ghatak, V.G. Rao, S. Mandal, N. Sarkar, Effects of 1-butyl-3-methyl imidazolium tetrafluoroborate ionic liquid on Triton X-100 aqueous micelles: solvent and rotational relaxation studies, J. Phys. Chem. B 115 (2011) 6957–6963.
[34] L.G. Chen, H. Bermudez, Solubility and aggregation of charged surfactants in ionic liquids, Langmuir 28 (2012) 1157–1162.
[35] S.P.M. Ventura, L.D.F. Santos, J.A. Saraiva, J.A.P. Coutinho, Ionic liquids microemulsions: the key to Candida antarctica lipase B superactivity, Green Chem. 14 (2012) 1620–1625.
[36] R. Sharma, S. Mahajan, R.K. Mahajan, Surface adsorption and mixed micelle formation of surface active ionic liquid in cationic surfactants: conductivity, surface tension, fluorescence and NMR studies, Colloids Surf. A Physicochem. Eng. Asp. 427 (2013) 62–75.
[37] C. Duran, D. Ozdes, V.N. Bulut, M. Tufekci, M. Soylak, Cloud-point extraction of Rhodamine 6G by using Triton X-100 as the non-ionic surfactant, J. AOAC Int. 94 (2011) 286–292.
[38] D. Blankschtein, G.M. Thurston, G.B. Benedek, Phenomenological theory of equilibrium thermodynamic properties and phase separation of micellar solutions, J. Chem. Phys. 85 (1986) 7268–7288.
[39] Y. Kohno, H. Ohno, Temperature-responsive ionic liquid/water interfaces: relation between hydrophilicity of ions and dynamic phase change, Phys. Chem. Chem. Phys. 14 (2012) 5063–5070.
[40] X. Wang, J. Liu, L. Yu, J. Jiao, R. Wang, L. Sun, Surface adsorption and micelle formation of imidazolium-based zwitterionic surface active ionic liquids in aqueous solution, J. Colloid Interface Sci. 391 (2013) 103–110.
[41] X. Qi, X. Zhang, G. Luo, C. Han, C. Liu, S. Zhang, Mixing behavior of conventional cationic surfactants and ionic liquid surfactant 1-tetradecyl-3-methylimidazolium bromide ([C14mim]Br) in aqueous medium, J. Dispers. Sci. Technol. 34 (2012) 125–133.
[42] V.C. Santos-Ebinuma, A.M. Lopes, A. Converti, A. Pessoa, C.de O. Rangel-Yagui, Behavior of Triton X-114 cloud point in the presence of inorganic electrolytes, Fluid Phase Equilib. 360 (2013) 435–438.
[43] H. Schott, A.E. Royce, S.K. Han, Effect of inorganic additives on solutions of nonionic surfactants: VII. Cloud point shift values of individual ions, J. Colloid Interface Sci. 98 (1984) 196–201.
[44] Y. Zhang, P.S. Cremer, Interactions between macromolecules and ions: the Hofmeister series, Curr. Opin. Chem. Biol. 10 (2006) 658–663.
[45] D. Keilin, E.F. Hartree, Purification and properties of cytochrome c, Biochem. J. 39 (1945) 289.

[46] ChemSpider – The free chemical database at http://www.chemspider.com (accessed March 2014).
[47] Y. Lu, W. Lu, W. Wang, Q. Guo, Y. Yang, Thermodynamic studies of partitioning behavior of cytochrome c in ionic liquid-based aqueous two-phase system, Talanta 85 (2011) 1621–1626.
[48] C.L.S. Louros, A.F.M. Cláudio, C.M.S.S. Neves, M.G. Freire, I.M. Marrucho, J. Pauly, J.A.P. Coutinho, Extraction of biomolecules using phosphonium-based ionic liquids + K_3PO_4 aqueous biphasic systems, Int. J. Mol. Sci. 11 (2010) 1777–1791.
[49] C.W. Ooi, C.P. Tan, S.L. Hii, A. Ariff, S. Ibrahim, T.C. Ling, Primary recovery of lipase derived from Burkholderia sp. ST8 with aqueous micellar two-phase system, Process Biochem. 46 (2011) 1847–1852.
[50] M. Amid, M. Abd Manap, M. Shuhaimi, Purification of a novel protease enzyme from Kesinai plant (*Streblus asper*) leaves using a surfactant–salt aqueous micellar two-phase system: a potential low cost source of enzyme and purification method, Eur. Food Res. Technol. 237 (2013) 601–608.